Thin Solid Films xxx (2011) xxx–xxx

Contents lists available at SciVerse ScienceDirect

Thin Solid Films

journal homepage: www.elsevier.com/locate/tsf

Deposition rate characteristics for steady state high power impulse magnetron sputtering (HIPIMS) discharges generated with a modulated pulsed power (MPP) generator☆

F. Papa [a,*], H. Gerdes [b], R. Bandorf [b], A.P. Ehiasarian [c], I. Kolev [a], G. Braeuer [b], R. Tietema [a], T. Krug [a]

[a] Hauzer Techno Coating BV, Van Heemskerckweg 22, 5928 LL, Venlo, The Netherlands
[b] Fraunhofer Institute for Surface Engineering and Thin Films IST, Bienroder Weg 54E, 38108 Braunschweig, Germany
[c] Materials and Engineering Research Institute, Sheffield Hallam University Howard St., Sheffield, S1 1WB, United Kingdom

ARTICLE INFO

Available online xxxx

Keywords:
HIPIMS
MPP
HIPP
High power impulse magnetron sputtering
Modulated pulse power
Highly ionized pulse plasma processes
Deposition rate
Chromium
Magnetic field

ABSTRACT

High power impulse magnetron sputtering (HIPIMS) pulses have been of great interest over the last decade. With such sputtering techniques a substantial amount of target material can be ionized and used for the engineering of surfaces and coatings. Depending on voltage, system configuration and target material, such discharges can be either transient or reach steady state currents during the pulse. The used HIPIMS power supply was a constant voltage supplies. Similarly, HIPIMS pulses with multiple steady state current phases can be generated using a modulated pulsed power (MPP) generator. A typical pulse consists of an ignition, low current and high current phase. The contribution of these phases to the deposition rate is presented. The ionization rate of single charge chromium ions has been found to increase linearly with increasing peak current density. An increase in deposition rate with lower magnetic field strength at the target surface can be attributed to a higher sputter yield due to a higher cathode voltage due to increasing system impedance in HIPIMS case, weaker trapping of deposition flux and to enhanced ion flux towards the substrate.

1. Introduction

Highly ionized pulse plasma processes (HIPP processes) have been of great interest over the past decade due to the fact that a substantial fraction of the sputtered target material can be ionized. The generation of these ionized sputtered species has opened the possibility to modify coating properties and to use self-assisted ion deposition for the deposition of industrial coatings for different applications [1–7]. Mozgrin [8] and Bugaev [9] are describing such discharges. However, most pulses which have been studied are of short duration (10–200 μs) and involve the application of very high power densities (>1000 W cm^{-2}). In some cases, these discharges during a single pulse have the characteristic of a transient current relationship with respect to time, not reaching any steady state or plateau until the end of the pulse. However, with appropriate voltages, steady state currents can be reached even if the pulse duration is short. There are two review articles [10, 11] which discuss the main characteristics of such pulses, therefore they will not be considered in detail here. Longer pulses generated with a constant voltage supply have been studied by Anders et al. [12]. These pulses exhibit the typical transient behavior in the beginning of the pulse followed by an increase in plasma impedance due to gas rarefaction. At lower voltages, materials such as titanium exhibit a steady state current phase following the ignition phase. If the voltage is high enough and the target material has the correct physical characteristics, copper for example, a self-sustained sputtering state in which the discharge current is constant can be achieved. One limitation of constant voltage supplies is that the voltage during the pulse cannot be increased or otherwise manipulated. By modulating the voltage with a series of "micropulses" during a "macropulse", the peak current at the cathode can be manipulated and adjusted to settle at distinct, nearly constant levels. Hopwood [13] has shown that the main ionization mechanism for highly dense plasmas like HIPIMS discharges is electron impact ionization. Therefore, the advantage of being able to control the peak current during the discharge is that the metal/gas ion ratio can be controlled, since a correlation between the optical emission line intensities and applied pulse current was reported by Bandorf et al. [14].

Aside from the peak current during the discharge itself, it has been shown that magnetic field strength and configuration play a significant role in the deposition rate and ion flux to the substrate. By weakening the tangential magnetic field strength at the target face, the flow of ionized metal flux to the substrate can be enhanced due to the weakening of the trapping effect of the magnetic field in front of the target [15] as observed using constant voltage power supplies. Using steering fields, the metal ion flux can be directed due to ambipolar

☆ Paper presented at the 38th International Conference on Metallurgical Coatings & Thin Films, May 2–6, 2011, San Diego, CA, USA.

* Corresponding author. Tel.: +31 77 3559781; fax: +31 77 3969798.
E-mail address: fpapa@hauzer.nl (F. Papa).

0040-6090/$ – see front matter © 2011 Elsevier B.V. All rights reserved.
doi:10.1016/j.tsf.2011.09.004

diffusion where the electrons follow the field lines, thus directing "dragging" the ions along with them [16].

Since electron impact ionization has been cited as the main mechanism for metal ion generation in high power pulsed sputtering processes, the plasma characteristics and deposition rate were analyzed with respect to the peak current at the cathode. Two magnetic field configurations were examined in order to investigate rate and ionization effects. In order to generate steady state peak currents, a modulated pulsed power (MPP) supply was used. A MPP pulse consists of a three phases: ignition, low ionization and high ionization [17]. By dissecting the pulse between the low and high ionization phases, the corresponding contributions of these phases to the deposition rate and plasma properties were characterized.

2. Experimental setup

2.1. Deposition technique

A Balzers BAS 450 sputtering system was used for the sputtering of chromium (Cr) with both a Z-Pulser SOLO 360 and an Advanced Energy 10 kW Pinnacle power supply. The machine was configured in a two cathode closed field unbalanced magnetron setup. One cathode with dimension 254 mm × 127 mm was used for deposition. Two magnetic field configurations were used, yielding 47 mT and 26 mT (maximum tangential component) of a balanced cathode, in order to examine the effects of magnetic field strength on the discharge characteristics. The tangential field strength was varied by retracting the magnet plate from the target. General modifications of the magnetic field and deposition rate were reported by Mishra et al. for similar setup [18].

The Z-Pulser SOLO 360 power supply was used to generate pulses of 1 ms duration. The output voltage was varied in ordered to control the peak cathode current. Discharge currents of 30–300 A, which result in current densities on the target surface of 0.1–1 A cm^2, were evaluated. The resulting current densities were calculated by the peak values, taking the full target area into account. The Advanced Energy supply was used for DC sputter deposition.

The system was pumped down to a base pressure of 1.5×10^{-3} Pa before all depositions. The Ar pressure was held constant at 5×10^{-1} Pa.

Due to the maximum output voltage of the SOLO-360 supply, it was only possible to reach a peak current density of 0.45 A cm^{-2} with the 26 mT magnetic field. Peak currents of 30 to 300 A were adjusted by reducing frequency from 65 to 11 Hz with increasing current to maintain an average power of 1 kW for all experiments.

For both magnetic field configurations, a weakly ionized plasma was generated for 500 μs (1st half pulse) followed by a transition to a more strongly ionized plasma for 500 μs (2nd half pulse).

2.2. Characterization techniques

An Intellemetrics IL150 quartz crystal thickness monitor was used to measure the deposition rate at a distance of 120 mm from the target. The cathode voltage was measured with a Tektronix P5200 500:1 voltage probe, whereas the cathode current was measured with a Hioki 2006 current probe. Time resolved Optical emission spectroscopy was performed with an AOS 4μchron spectrometer from IFU Diagnostic Systems GmbH. The unit has a spectral resolution from 0.05 nm at 250 nm up to 0.5 nm at 800 nm. The optical signals were sampled with a 1 μs time resolution. The optical fiber was oriented so that it faced the racetrack of the target at an angle of 30° to the surface plane. The fiber was kept clean by using 10 sccm of argon (Ar) as a purge gas through a tube encasing the fiber.

2.3. Analysis methods

Since the sputter yield is proportional to the square root of the energy of the incoming ions, there is a non-linear relation between the target voltage and the sputter yield. Emmerlich et al. [19] have shown that the sputter yield loss effect can be estimated according to

$$\rho = K^{-1/2} \tag{2}$$

where ρ is proportional to the deposition rate and K is the ratio of the pulsed cathode voltage to that of the DC voltage. Eq. (2) was used to calculate the deposition rate as related to this yield loss effect.

3. Results and discussion

3.1. Discharge characteristics

Typical discharge current and voltage waveforms are shown in Fig. 1. Following the initial ignition (from 0 to 100 μs) of the discharge with a peak cathode current density of approximately 0.2 A cm^{-2}, a discharge with a peak cathode current density of approximately 0.1 A cm^{-2} is held for 400 μs until the peak cathode current density is then increased to approximately 1 A cm^{-2} for the remaining 500 μs of the pulse. We refer to the current during the last 500 μs of the pulse as the peak current in the rest of the paper.

The ignition peak shows the discharge current is following the discharge voltage. The decrease in cathode voltage during the ignition phase is due to the design of electronics of the power supply. It is also evident that the plasma impedance is changing during the ignition phase until the current starts to flow. Following this initial drop in current, the voltage is again increased at 100 μs by the applied voltage micro pulses in order to maintain the cathode current. To maintain a nearly constant current in the second, high ionized phase of the macro pulse the cathode voltage is slightly increased by the voltage micro pulses forming the complete pulse sequence. However, there is an effect of the voltage oscillations with respect to the current sustenance during the pulse, but the study of the voltage oscillations falls beyond the scope of this analysis and will be the focus of future publications.

We will focus on the relationship between the peak current and deposition rate at different magnetic fields.

3.2. Current/voltage characteristics

For magnetron discharges, there exists a relationship between discharge current and discharge voltage [20].

$$I = kV^n \tag{1}$$

Here, k is a geometrical constant and n is mainly a function of the plasma impedance. For discharges with low plasma impedance (many available charge carriers in front of the target), n will have

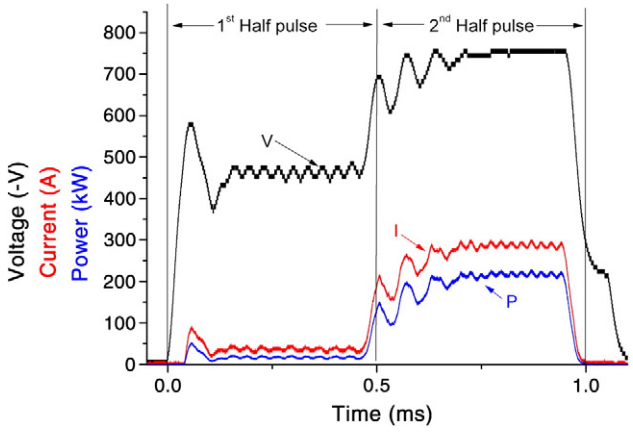

Fig. 1. Representative current/voltage/power vs. time characteristic for MPP pulse.

Please cite this article as: F. Papa, et al., Thin Solid Films (2011), doi:10.1016/j.tsf.2011.09.004

values greater than 3 (depending on target material and sputtering gas). When plasma pressure builds up to overcome magnetic field confinement, as in highly ionized HIPIMS process as described by Brenning et al. [21], n will approach a value of 1 [22].

Fig. 2 shows the average peak current versus the average peak voltage during the second half of the pulse. The I–V curve for the 47 mT field strength shows the typical impedance shift for HIPIMS type discharges. The transition to a high impedance plasma can be seen at approximately 200 A (0.6 A cm^{-2}), where the n changes suddenly from 8 to 4. Similar values have been reported in the literature [23]. This kink is caused partially by the loss of secondary electron confinement, resulting in a loss of available charge carriers. At 26 mT, the kink shifts to a much lower peak current, 80 A (0.25 A cm^{-2}). Here n changes from 5 to 2. This is most likely the result of the loss of electron confinement due high plasma density and also the weaker magnetic field confinement in general. As the cathode voltage is increasing rapidly after the inflection point, the electrons may escape the magnetic trap more easily due to their higher energies. Another mechanism which contributes to the change in impedance is the change in ion species available for sputtering. As the gas rarefaction occurs and the Cr^{1+} ions begin to become a more dominant species in front of the cathode, the impedance increases due to that fact that these Cr^{1+} ions do not have enough potential energy to release as many secondary electrons from the target surface as the Ar^{1+} and Cr^{2+} ions will do [24, 25].

3.3. OES data

In order to look at the amount of Cr^{+} ions in the plasma, the line intensity at 283.534 nm was examined. This line was chosen due to its high relative intensity and the lack of any corresponding chromium neutral or argon lines in the same vicinity.

It can be seen (Fig. 3) that the intensity of this Cr^{+} line follows the cathode current. The intensity of the line increases and decreases with the corresponding shift in peak cathode current.

By plotting the peak optical emission intensity for this line (corresponding to the second half of the pulse) against the peak cathode current density, Fig. 4, it can been seen that the trend is nearly linear indicating an increase of ions proportional to the increase in pulse current. In order to better fit the optical emission data, an adjacent-averaging function was employed. Noteworthy here, is that there is a linear correlation for single charged chromium emission intensity and cathode peak current density, regardless of the magnetic field strength.

This is to be expected since the main ionization mechanism for ionizing the sputtered target material is electron impact ionization [13], especially after passing a certain threshold value [14]. It should be noted that the fiber is looking through the plasma at the racetrack

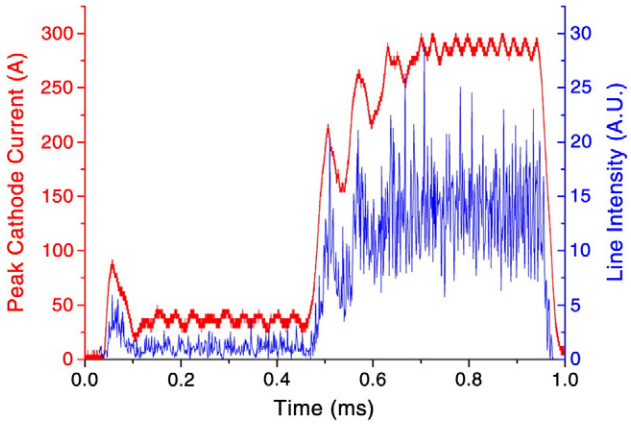

Fig. 3. Current characteristic and the corresponding measured optical intensity of Cr^{+} (283.534 nm).

itself, thereby giving us information concerning the discharge characteristics, but without spatial resolution.

3.4. Deposition rate

3.4.1. Full pulse consideration

The deposition rate versus peak cathode current density is shown in Fig. 5. For both field strengths, we can see a significant drop in deposition rate as compared to DC. At a peak current density of approximately 0.1 A cm^{-2}, the drop in deposition rate is approximately 30% and 50% for the 26 mT and 47 mT fields respectively. The data for the 47 mT depositions suggests that a plateau is being reached at about 25% of the DC rate. This change in deposition rate with magnetic field corresponds well to values reported in the literature for HIPIMS discharges with constant voltage [15].

There are several mechanisms which contribute simultaneously to the loss of deposition rate in HIPIMS type discharges. These mechanisms are the yield loss effect, metal ion return effect, plasma confinement due to the magnetic trapping effect and change in directional flux due to cross field ion transport. It is fair to say that it is extremely difficult to determine experimentally the contribution from each of the above mentioned loss effects with high precision. A model for some of the loss mechanisms was proposed by Christie [26] and further improved by Vlcek [27].

Measurement of deposition rate for the two magnetic configurations is plotted in Fig. 5 together with curves calculated based on Eq. (2) compensating for the yield loss effect. A time average voltage was used for this calculation as the voltage varies significantly during

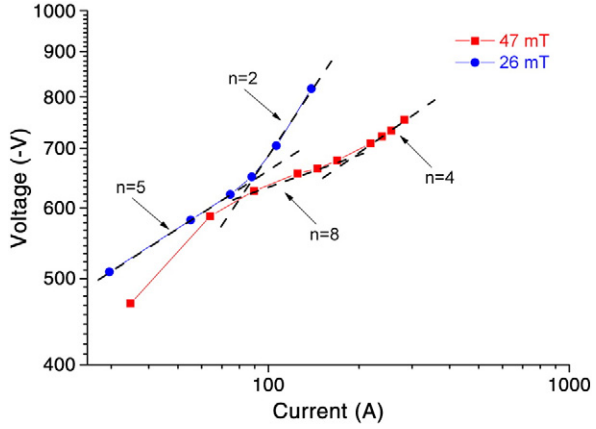

Fig. 2. Current/voltage characteristics for 47 mT and 26 mT field strengths.

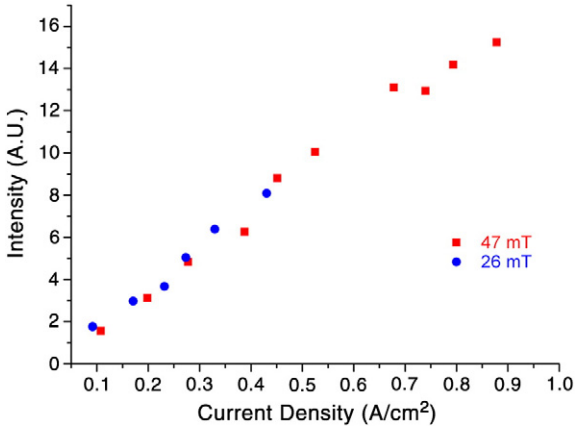

Fig. 4. OES emission intensity vs. peak cathode current density for 283.534 nm Cr^{+}.

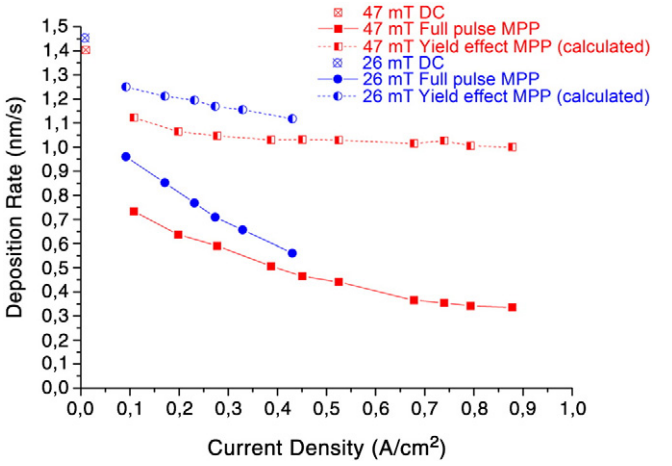

Fig. 5. Deposition rate vs. peak cathode current density. The half full symbols represent the calculated loss in deposition rate due to the yield effect.

the three phases of the pulse itself. The deposition rate plotted over peak current for the different magnetic configurations appears to have two different slopes. This is mainly a result of the faster increase in target voltage for the 26 mT case. This data shows that the drop in deposition rate resulting from the yield effect as compared to the DC rate at 0.1 A cm^{-2} is 14% and 20% for 26 mT and 47 mT respectively. At 0.45 A cm^{-2}, the loss would be 23% for the 26 mT field. At 0.9 A cm^{-2}, the reduction is 29% for the 46 mT field.

By comparing the calculated yield curve and the actual deposition rate, the rate loss due to the magnetic confinement, return and directional loss effects can be estimated. These effects account for a 20% and 28% loss in deposition rate at 0.1 A cm^{-2} for the 26 mT and 47 mT fields respectively. At 0.45 A cm^{-2} for the 26 mT field strength, the loss due to the yield effect is 39%. For the 47 mT field strength, the loss is 47%. These values represent the "real" decrease in deposition rate due to the loss of ion flux reaching the substrate, by either redirecting the ions to the target for resputtering or sideway transport.

It is expected that the absolute number of ions not arriving at the substrate due to magnetic confinement and return effects will increase with increasing peak current density and increasing magnetic field strength, as both will increase the metal ion density and affect location of ion formation.

These effects will play an important role even at relatively low peak current densities (0.1 A cm^{-2}), since we have verified the noticeable existence of Cr^{1+} in the plasma. It has also been reported elsewhere, that the amount of ionized Cr is significant, even at low to moderate peak current densities [17]. Likewise shown for titanium [14] the Cr-ionization increases with the plasma density, as seen in Fig. 3 where the emission intensity follows the current modulations in the pulse.

Lundin [28] has shown that another mechanism contributing to the loss of deposition rate is due to the fact that some of the sputter target material is accelerated and transported radially away from the cathode. This work was done with a peak current density of 6 A cm^2. It should only be mentioned here that this is a possible mechanism for the deposition rate loss even at moderately low peak current densities.

3.4.2. Pulse segment contributions

Since we are using a multiple stage pulse, the individual contributions of the pulse segments to the overall deposition rate deserve attention (Fig. 6). The deposition rate for the first half of the pulse was determined by programming a 500 μs pulse with the same discharge behavior as the first half of the 1000 μs pulses being studied here (see Fig. 1). Knowing this rate, the contribution to the total deposition rate from both pulse "halves" can be calculated. The contribution of the high current segment of the pulse can be seen to become quickly predominant. For the 47 mT field strength, the segment rates suggest that a plateau is being reached for high currents. We expect that this is due to the formation of more Cr^{2+} ions in the plasma. Therefore the same ion current either will be realized by a smaller number of 2+ ions than 1+ ions required for that current. These double charged ions will then sputter the target, if redirected with twice the energy. Or the increased secondary electron emission will compensate the higher ionization resulting in a lower ion current.

The increase in Cr^{2+} as a function of peak current density has been reported in the literature [15, 22]. It cannot be said that such a plateau is being reached for the 26 mT field strength, as we were not able to gather more data in the higher peak current density range due to power supply limitations. As the peak current density is increased, the contribution of the first half pulse for the 26 mT field does not vary significantly from that of the first half pulse rate for the 47 mT field. This suggests that relative contribution of the lower peak current segment of the pulse is approximately the same for both field strengths and is absolutely significantly less for the 26 mT field strength. As the peak power in the "2nd half pulse" increases, the pulse frequency has to decrease in order to maintain 1 kW average power on the cathode. This results in an apparent drop in deposition rate for the "1st half pulse" curve. The loss of rate seen in the "2nd half pulse" curve is due to the loss of ion flux towards the substrate.

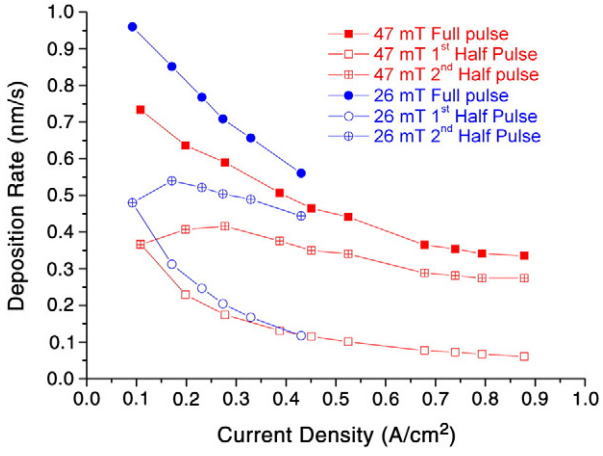

Fig. 6. Deposition rate vs. peak cathode current density. Figure shows the individual contributions to the deposition rate of the low and high ionization segments of the pulse. The lower curves sum to the value of the overall deposition rate (upper curves).

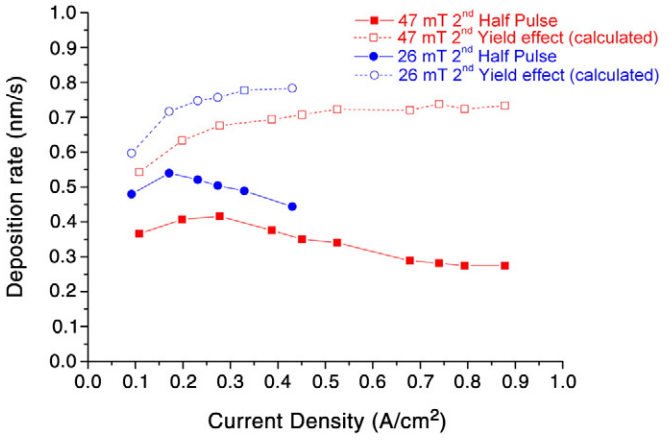

Fig. 7. Deposition rate contribution from the second half of pulse vs. peak cathode current density. Calculated rate curves accounting for yield effect are also shown.

Please cite this article as: F. Papa, et al., Thin Solid Films (2011), doi:10.1016/j.tsf.2011.09.004

3.4.3. "Higher" ionization pulse segment

To further examine this point in more detail, the relationship between magnetic field (Fig. 7) and the peak current density was observed, now taking the yield loss calculation into account. As only the second half of the pulse is evaluated here, it must be considered that only this fraction of the peak power contributes to the average power, thus the yield effect data has been normalized to take into account that the contribution to the deposition rate of the second half of the pulse becomes more significant as peak current density is increased. The initial increase is caused mainly by contribution of the low ionization. With increasing peak current the deposition rate in the second half of the pulses at both magnetic field strength first increases to a given peak current density. After reaching a maximum the deposition rate drops due to significant increase of ionization and the connected loss mechanisms. Therefore the rate drop starts at 0.18 A cm^{-2} for the 26 mT field strength and at 0.28 A cm^{-2} for the 47 mT field strength, respectively. The difference between the curves reflects the loss of Cr ions either to the confinement and return effects or to a change in the directional flux of the sputtered atoms with respect to the target surface. This effect becomes much more pronounced above the mentioned inflection points.

When comparing the ratio of calculated yield values to the actual deposition rate values, it appears that there is an extra component of the higher deposition rate at the lower field strength which must be taken into account. After accounting for yield effect, the deposition rate at 26 mT is 13% higher at 0.1 A cm^{-2} and 7% higher at 0.45 A cm^{-2} than for the 47 mT field. This most likely corresponds to lower return probability of ions for lower magnetic fields. This results in a higher metal ion flux to the substrate.

4. Conclusions

A comparison of steady state HIPIMS discharges driven by a MPP power supply has been made for two tangential magnetic field strengths, 46 mT and 26 mT. The impedance of the plasma is found to increase as a function of increasing peak current density and behaves in a similar manner to that of typical HIPIMS discharges. The onset of the impedance increase occurs at a markedly lower value, 0.25 A cm^{-2}, for the 26 mT magnetic field than for the 47 mT field, 0.6 A cm^{-2}. It has been confirmed that the flux of the Cr ions increases linearly as a function of peak current density at the cathode and is independent of the magnetic field strength. The deposition rate for both field strengths is found to be lower as compared to DC rates and decreases with increasing peak current density. The contribution of the deposition rate from the low and high ionization phases of the pulse has also been determined. As the peak cathode current is increased, the contribution to the sputtered flux from the high ionization phase becomes dominant. The trend for both magnetic fields strengths is similar. It can be seen that the deposition rate for the 26 mT field strength is 17–30% higher than that for the 47 mT field strength. At the same time the plasma composition is modified, and the lower field will mainly consist of single charged, while the stronger field also will generate higher charged ions. This rise and offset in deposition rate for the lower, 26 mT field strength, are a result of the yield effect, since the discharge is running at higher voltages, the weakening of the trapping effect of the magnetic field in front of the target, and lower return probability of the metal ions. A slight rise in deposition rate at low peak current densities has also been seen. Regulating the magnetic field strength presents a useful tool for enhancement of the deposition rate in HIPIMS as this has been shown to be effectively independent from the design of the power supply.

Role of the funding source

An STSM grant has been given for this study. The role of the funding source has been purely financial. They had no role in study design, collection, analysis or interpretation of data. The funding source also played no role whatsoever in the writing of the report or the decision to submit the paper for publication.

Disclosure statement

All authors state that there are no potential conflicts of interest including any financial, personal or other relationships with other people or organizations that could have influenced the work submitted in this paper. All authors participated in the research or article preparation and they have all approved the final article.

Acknowledgments

The author would like to thank the COST Action MP0804 "Highly Ionised Pulse Plasma Processes — HIPP Processes" for supporting this research within a STSM grant.

References

[1] J. Alami, P.O.A. Persson, D. Music, J.T. Gudmunsson, J. Bohlmark, U. Helmersson, J. Vac. Sci. Technol. A 23 (2005) 278.
[2] K. Bobzin, N. Badcivan, P. Immich, S. Bolz, J. Alami, R. Cremer, J. Mater. Process. Technol. 209 (2008) 165.
[3] R. Chistyakov, B. Abraham, W.D. Sproul, J. Moore, J. Lin, Society of Vacuum Coaters 50th Annual Technical Conference Proceedings, Louisville, KY, 2007, p. 139.
[4] A.P. Ehiasarian, J.G. Wen, I. Petrov, J. Appl. Phys. 101 (2007) 054301.
[5] A.P. Ehiasarian, W.-D. Munz, L. Hultman, U. Helmersson, I. Petrov, Surf. Coat. Technol. 163–164 (2003) 267.
[6] P.E. Hosvepian, C. Reinhard, A.P. Ehiasarian, Surf. Coat. Technol. 201 (2006) 4105.
[7] V. Kouznetsov, K. Macak, J.M. Schneider, U. Helmersson, I. Petrov, Surf. Coat. Technol. 122 (1999) 290.
[8] D.V. Mozgrin, I.K. Fetisov, G.V. Khodachenko, Plasma Phys. Rep. 21 (1995) 401.
[9] S.P. Bugaev, N.N. Kovel, N.S. Sochugov, A.N. Zakharov, XVIIth International on Discharges and Electrical Insulation in Vacuum, 1996, p. 1074.
[10] K. Sarakinos, J. Alami, S. Konstantinidis, Surf. Coat. Technol. 204 (2010) 1661.
[11] U. Helmersson, M. Lattemann, J. Bohlmark, A.P. Ehiasarian, J.T. Gudmunsson, Thin Solid Films 513 (2006) 1.
[12] A. Anders, J. Andersson, A.P. Ehiasarian, J. Appl. Phys. 102 (2007) 113303.
[13] J.A. Hopwood, in: J.A. Hopwood (Ed.), Thin Films: Ionized Physical Vapor Deposition, Academic Press, San Diego, 2000, p. 181.
[14] R. Bandorf, M. Vergöhl, K. Schiffmann, T. Wallendorf, Society of Vacuum Coaters 49th Annual Conference Proceedings, Washington, DC, 2006, p. 21.
[15] A.P. Ehiasarian, A. Vetushka, Society of Vacuum Coaters 52nd Annual Conference Proceedings, Santa Clara, CA, 2009, p. 265.
[16] J. Bohlmark, M. Oestbye, M. Lattemann, H. Ljungcrantz, T. Rosell, U. Helmersson, Thin Solid Films 515 (2006) 1928.
[17] J. Lin, J.J. Moore, W.D. Sproul, B. Mishra, J.A. Rees, Z. Wu, R. Chistyakov, B. Abraham, Surf. Coat. Technol. 203 (2009) 3676.
[18] A. Mishra, P.J. Kelly, J.W. Bradley, Plasma Sources Sci. Technol. 19 (2010) 045014.
[19] J. Emmerlich, S. Mráz, R. Snyders, Kaiyun Jiang, J.M. Schneider, Vacuum 82 (2008) 867.
[20] S.M. Rossnagel, H.R. Kaufman, J. Vac. Sci. Technol. A A6 (2) (1988) 223.
[21] N. Brenning, R.L. Merlino, D. Lundin, M.A. Raadu, U. Helmersson, Phys. Rev. Lett. 103 (2009) 225003.
[22] A.P. Ehiasarian, R. New, W.-D. Munz, L. Hultman, U. Helmersson, V. Kouznetsov, Vacuum 65 (2002) 147.
[23] J. Alami, K. Sarakinos, G. Mark, M. Wuttig, Appl. Phys. Lett. 89 (2006) 154104.
[24] A. Anders, J. Andersson, A.P. Ehiasarian, J. Appl. Phys. 103 (2008) 039901.
[25] A. Anders, Appl. Phys. Lett. 92 (2008) 201501.
[26] D.J. Christie, J. Vac. Sci. Technol. 23 (2005) 330.
[27] J. Vlcek, K. Burcalova, Plasma Sources Sci. Technol. 19 (2010) 065010.
[28] D. Lundin, P. Larsson, E. Wallin, M. Lattemann, N. Brenning, U. Helmersson, Plasma Sources Sci. Technol. 17 (2008) 035021.